Rev. Roum. Sci. Techn.– Électrotechn. et Énerg.
Vol. **69**, *1*, pp. 55–60, Bucarest, 2024

PERFORMANCE INVESTIGATION OF SINGLE-PHASE TRANSFORMERLESS PV INVERTER CONNECTED TO LOW VOLTAGE NETWORK

SALIHA BOULAHCHICHE[1, 2], AMAR HADJ ARAB[2], SALIM HADDAD[1], ISMAIL BENDAAS[2], SALIM BOUCHAKOUR[2], ABDELHAK RAZAGUI[2]

Keywords: Grid-connected photovoltaic (PV) system; Transformerless PV inverter; Galvanic isolation; Leakage current; Insulation resistance.

Due to their high efficiency and reduced size and weight compared to transformer-based inverters, transformerless single-phase inverters are the most widely used in photovoltaic systems connected to the low-voltage grid. Unfortunately, the absence of galvanic isolation leads to ground faults caused by capacitive leakage current flow and deterioration of the inverter's insulation resistance on the dc side. This paper examines the performance of the three transformerless single-phase inverters of the first grid-connected photovoltaic system in Algeria under adverse weather conditions, such as rain, as there is no galvanic isolation between the dc and ac side of the inverter, making operation of the photovoltaic system more difficult. The flow of capacitive leakage current from the earth to the inverter output is one of the two phenomena, resulting in protection devices being triggered involuntarily. The second phenomenon is system shutdown due to a decrease in the inverter's insulation resistance at the input. The VDE 126-1-1 standard integrated into the inverter, which defines the safety requirements for grid-connected photovoltaic systems, is used in this article to manage and analyze both phenomena.

1. INTRODUCTION

Renewable energy has emerged as a vital component in energy systems, serving as a potent source for energy production and offering a promising avenue to mitigate the adverse impacts of pollution. The imperative to combat global warming has led to adopting green energy policies, encouraging the integration of renewable energy systems to meet rising electricity demands and reduce greenhouse gas emissions. Photovoltaic (PV) energy, due to its cost-effectiveness in implementation and maintenance, stands out as an attractive option. Presently, the predominant application of solar PV involves grid-connected setups, wherein PV modules are linked to the electrical grid through devices such as grid-connected inverters [1,2–6].

Algeria, known as one of the sunniest regions globally, holds immense solar potential, with a satellite assessment by the German Aerospace Center (DLR) indicating the highest solar potential in the Mediterranean basin at 169,440 TWh/year [9]. The country experiences an average annual daily sunshine ranging from 5 to 6 kWh/m^2/day, translating to approximately 1,700 kWh/m^2/year for the North and 2,650 kWh/m^2/year for the South. Coupled with a substantial underground water reservoir and diverse climatic conditions, Algeria's southern region exhibits cold winters and scorching summers, with average temperatures ranging from around 10.7 °C in January to 34 °C in July [7]. In alignment with environmental goals, the Algerian government has initiated a national program targeting a total renewable capacity of 22 GW by 2030, aiming to curtail approximately 193 million tonnes of CO2 emissions [19].

Within grid-connected PV systems, inverters play a pivotal role, converting direct current (dc) from PV grids into alternating current (ac) sources [8]. Inverters can be broadly categorized as isolated and non-isolated based on galvanic isolation. While isolated inverters incorporate transformers to enhance dc output voltage matching with ac voltage, they suffer from reduced overall efficiency and increased system size and losses. Transformer-less inverters, particularly single-phase ones, are lauded for their high efficiency, compact size, low cost, and lightweight. However, the absence of galvanic isolation in these inverters leads to conduction loops, capacitive leakage currents, and potential issues related to insulation resistance degradation, affecting power quality, and causing electromagnetic emissions and harmonics in the electrical infrastructure [10].

This study delves into the performance analysis of three single-phase transformer-less inverters, focusing on the intricate interplay between insulation resistance challenges and capacitive leakage current in line with the DIN VDE 0126-1-1 standard. The investigation unfolds through results from a meticulous measurement campaign conducted in a 9.54 kWp photovoltaic system seamlessly integrated with the grid, situated at the Renewable Energy Development Center (CDER) in Algeria. Our exploration seeks to unravel the complexities surrounding the interrelationship between insulation resistance and capacitive leakage current in monophasic photovoltaic inverters without transformers.

The paper is organized as follows: section 1 presents the introduction, section 2 covers leakage current analysis, section 3 discusses Insulation resistance analysis, section 4 details location characteristics, material, and methodology, section 5 presents results and discussions, and the findings are summarized in section 6.

2. LEAKAGE CURRENT

Photovoltaic systems employing transformer-less inverters (TL) may generate leakage currents because of the capacitive traits of the panels and the absence of galvanic isolation between the dc and ac components. These capacitors, when exposed to an ac component in the dc circuit, produce leakage currents in the grounding terminal, potentially reaching hazardous levels upon direct contact with the ground wire (see Fig. 1) [12,13]. In the first scenario, this results in a momentary disconnection of the inverter from the public grid. In contrast, in the second

[1]LGMM Laboratory, Université 20 août 1955-Skikda, PB N◦ 26 Route Elhadaik, 21000 Skikda, Algeria
[2]Centre de Développement des Energies Renouvelables BP. 62, Route de l'Observatoire Bouzareah, 16340 Algiers, Algeria
E-mails: boulahchiche21@live.com, a.hadjarab@cder.dz, s.haddad@univ-skikda.dz, s_bendaas@hotmail.fr, s.bouchakour@cder.dz, a_razagui@yahoo.fr

DOI: 10.59277/RRST-EE.2024.69.1.10

scenario, grid feed interruption occurs until the manual reactivation of the residual current device (RCD) in the feeder cable (see Fig. 1) [11]. The physical properties of the displacement current (I) can be elucidated as follows.

$$I = \frac{\Delta Q}{\Delta t} = C\frac{\Delta U}{\Delta t} = 2\pi f C U, \quad (1)$$

where C is the parasitic capacitance, I is the capacitive leakage current, and f is the network frequency.

2.1. COMMON MODE VOLTAGE

Without a transformer, the grid ground and the photovoltaic field lack a galvanic connection, forming a common-mode resonant circuit [10,12]. The ac voltage CM, predominantly influenced by the topology structure and control approach, can activate the resonant circuit, causing a significant ground leakage current. This common-mode voltage may stem from the topology structure and modulation scheme of the harmonic filter (LC) [10,12,13]. The correlation of the common-mode voltage can be articulated as follows:

$$V_{CM} = \frac{1}{2}(V_{AN} + V_{BN}), \quad (2)$$

where V_{CM} is the RMS value of the ac voltage at the photovoltaic inverter (common mode voltage), V_{AN} and V_{BN}. The controlled voltage source is connected to the neutral N.

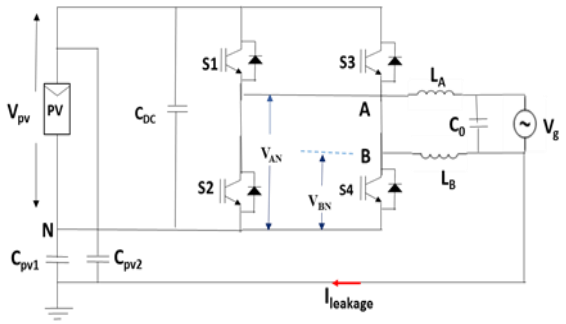

Fig. 1 – Grid-tied H-bridge PV inverter.

Our chosen topologies for full bridge SMA inverters, HERIC and H5, widely used in commercial applications, effectively reduce leakage current by integrating a single switch with an H-bridge inverter [11,13]. The transformerless single-phase H5 inverter, with its advanced design optimizing efficiency in single-phase systems, tackles capacitive leakage current challenges associated with the absence of galvanic isolation. By eliminating the need for a transformer, the H5 inverter minimizes size, weight, and costs while introducing innovative solutions for capacitive leakage current mitigation. This signifies a significant advancement, providing high performance and improved capacitive leakage current management, making the H5 inverter an efficient and reliable energy solution for single-phase applications.

2.2. PARASITIC CAPACITANCES

The occurrence of leakage current in photovoltaic (PV) systems is highly contingent on the parasitic capacitance between the PV panel and the ground. The PV module generates an electrically rechargeable surface juxtaposed with a grounded frame [11,12]. This parasitic capacitance is influenced by diverse factors, including the solar panel and frame structure, cell surface, cell distance, meteorological conditions, humidity, dust or salt accumulation on the panels, and the earth's resistance value [11,12]. The parasitic capacitances can be categorized as cell-image capacitance (C_{cf}), cell-rack capacitance (C_{cr}), and cell-earth capacitance (C_{cg}) [12]. The intrinsic performance of a panel is intricately tied to the surrounding components, such as glass, ethylene-vinyl acetate (EVA), back sheet (Tedlar), and aluminum frame. Additionally, capacity determination is significantly influenced by associated elements like the panel frame, mounting support, or ground, all serving as determinants of capacitive potential (see Fig. 2).

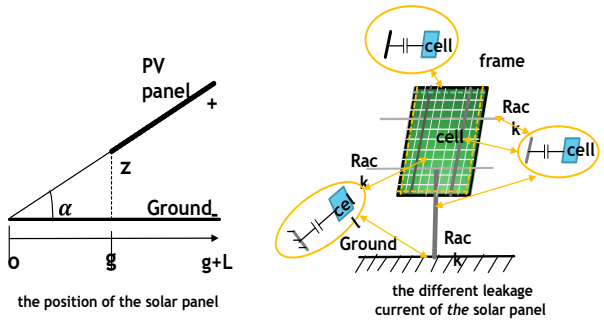

Fig. 2 – The method of calculating the capacitance capacity.

$$C = C_{cf} + C_{cr} + C_{cg}, \quad (3)$$

$$C_{cf} = C_{cr} = \frac{\varepsilon_0 \varepsilon_r L_r W_f}{T} = C_{in}, \quad (4)$$

$$C_{cg} = \frac{\varepsilon}{\alpha} \ln \frac{L_{pv}+g}{g}, \quad (5)$$

$$g = \frac{z}{\tan\alpha}, \quad (6)$$

where C_{in} is the inner-cell coupling capacity, ε_0 is the dielectric vacuum permittivity, ε_r is the relative permittivity of the dielectric between the cell and the aluminum strip, L_r is the length of the aluminum strip, W_r is the width of the aluminum strip, T is the distance between the rack and the cell, z is the mounting height and α is the angle between PV panel and ground.

2.3. NEURAL REGIME AND CHOICE A RESIDUAL DIFFERENTIAL CURRENT DEVICE

In Algeria, the TT regime involves grounding the power supply neutral and installation masses, with a mandatory differential current device monitoring residual current. According to DIN VDE 0126-1-1 standards, the permissible leakage current is 30 mA, typically triggering between 15 to 30 mA. Using the Chauvin ARNOUX CA6116 controller, tests examined the sensitivities of three differentials at the output of three inverters, establishing a correlation between sensitivity and leakage current passage. Table 1 shows the current-time relationship, pinpointing distinct sensitivities and their impact on leakage current passage.

Table 1
Sensitivity three differential circuit breakers

	Disjunction current (mA)	disjunction time (mS)
Differential n°1	22.7	12.5
Differential n°2	20.1	11
Differential n°3	21.8	32.9

3. THE INSULATION RESISTANCE

In a photovoltaic system, the interconnected insulation resistances (Riso) of photovoltaic modules form a parallel connection to the ground, reducing the overall earth resistance. This reduction becomes a challenge when

connecting the inverter to the grid, potentially rendering the entire PV system unsuitable for grid connection despite correct component functioning. For transformer-less inverters without galvanic separation, compliance with standards like DIN VDE 0126-1-1 requires Riso to be above 1 kΩ/V, with a minimum of 500 kΩ. The inverter actively monitors insulation resistance throughout the system, covering photovoltaic modules, dc cables, the overall system, and the inverter itself. This vigilance is crucial as a single short circuit can cause material damage and personal injury. Additionally, insulation resistance to the ground depends on factors like the technology of the photovoltaic module and inverter, grid size, specific insulation properties, and the series resistance of the EGC. The specified insulation resistance value is determined by eq. (7), considering multiple factors [10–14,17]

$$R_{iso} = \frac{1}{\frac{S.M}{R_{module}} + \frac{1}{R_{inv}} + \frac{1}{R_{fault}}} + R_{EGC}, \quad (7)$$

where R_{module} is the isolation of module, R_{inv} is the inverter isolation, R_{fault} is the fault resistance, S is the number of strings in the array, M is the number of modules in a string, and R_{EGC} is the equipment ground conductor (EGC) resistance.

The insulation resistance requirement for 1 m² PV panel, as per DIN EN 61646 and DIN IEC 61215, is a minimum of 40 MΩ. When connected to an inverter, the parallel connection of insulation resistances from multiple photovoltaic panels decreases the overall resistance of the photovoltaic system to Earth [12–17]

$$R_{iso} = \frac{1}{\frac{1}{\text{module}_1} + \frac{1}{\text{module}_2} + \cdots + \frac{1}{\text{module}_n}}, \quad (8)$$

$$R_{iso} = \frac{R_{iso}\ Panels}{\text{number of panels}}. \quad (9)$$

R_{iso} measurements on ungrounded systems involve injecting a voltage pulse from an external power source. Ground isolation can be calculated by analyzing the current drawn from the power source, as expressed in:

$$R_{iso} = \frac{V_{applied}}{I(V_{applied}) - I(V_{applied}=0)}. \quad (10)$$

4. HARMONIC ANALYSIS

Power grids ' primary goal is ensuring user safety while supplying electricity, aligning with EN 50160 and other power quality regulations. Inverters provide grid-connected PV systems as power electronic devices with non-sinusoidal output voltages and currents. Analyzing power network issues causing harmonic voltage dips is crucial due to the increasing significance of harmonic distortion [2–5].

Figures 3 and 4 illustrate voltage and current THD for each inverter at varying solar power penetration levels. Lower solar irradiation levels result in a notable total current THD from the inverters. In the 600 to 650 W range (25 % of RMS power values relative to rated power), the current THD remains below 5 %. Importantly, there is a direct correlation between connected loads, PV output power, and voltage THD.

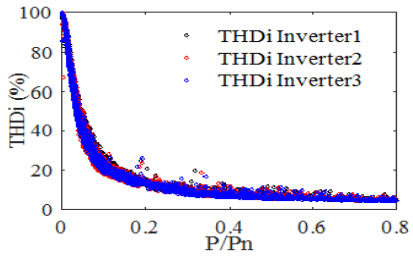

Fig. 3 – Total current harmonic profiles.

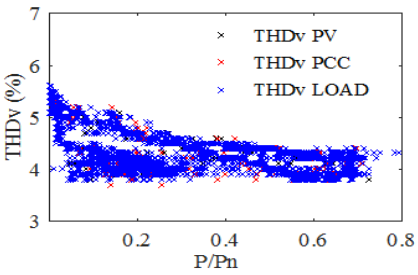

Fig. 4 – Total voltage harmonic profiles.

5. LOCATION, MATERIAL AND METHODOLOGY

Figure 5 showcases the 9.45 kW PV system with 90 Isofoton PV modules organized into three subsystems connected to the grid through three SMA Sunny Boy 3000TLST-21 inverters. Each subfield has two parallel strings of 15 modules linked in series to Sonelgaz's 230 V, 50 Hz grid, ensuring safety with dc protection between the PV panel and the inverter and ac protection between the inverter and the grid [19].

5.1. DATA MEASUREMENT AND MONITORING

In the research lab, measurements of the PV system connected to the grid were taken at the inverter's input and output.

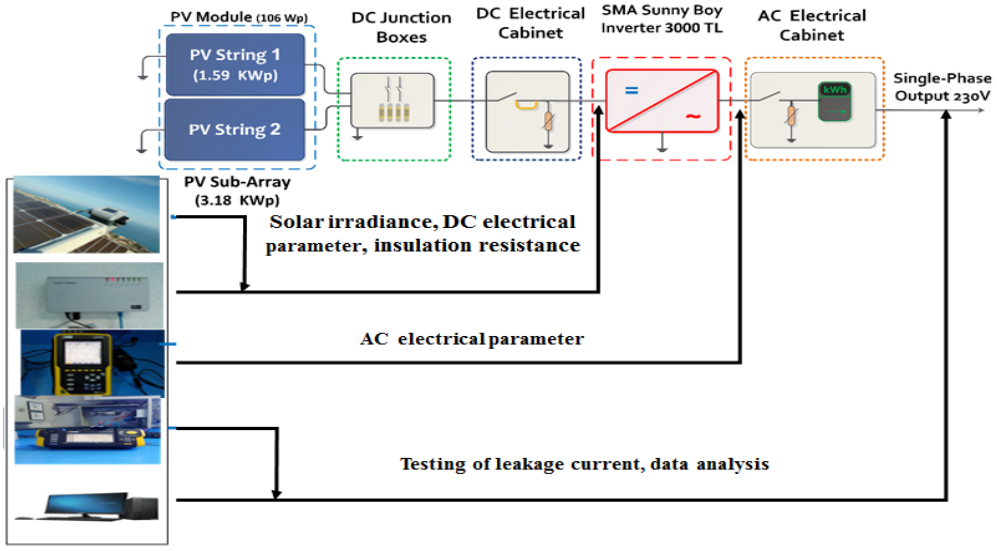

Fig. 5 – System diagram connected to the CDER network.

Electrical characteristics and insulation resistance (DIN VDE 0126-1-1 compliant) at the inverter's input were measured using data from Sunny WebBox, Sunny Portal, and the Chauvin ARNOUX CA6116 electrical network controller. Climatic data is recorded by the Sunny Sensor Box on each PV module. The inverter's output parameters (active power, THD of current and voltage, and efficiency) were measured with one-minute resolution using a Chauvin Arnoux C.A8335. Figure 5 also illustrates the research phases and tools for examining the impact of sampling on inverter performance.

6. RESULTS AND DISCUSSIONS

This section covers power efficiency, current, and voltage THD and compares insulation resistance degradation and capacitive leakage current flow across the three PV subsystems. Figures 6–11 display data from Sunny WebBox and Chauvin Arnoux C.A8335 network analyzer, while Figs. 13, 14 depict Sunny Portal data.

6.1. INVERTER EFFICIENCY

Figure 6 illustrates the variations in efficiency among the three inverters concerning output active power, as per the European model. At 300 W active power, the maximum inverter efficiency is 98 %.

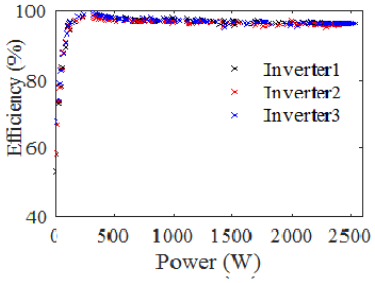

Fig. 6 – Inverter efficiency against solar radiation.

6.2. LEAKAGE CURRENT AND INSULATION RESISTANCE

Figure 7 illustrates the photovoltaic power variation of the first inverter on a rainy day and in sunlight. The inverter remains inactive for about an hour between 8:00 and 9:00 due to insulation resistance degradation. Figure 10 (Riso1) depicts the resistance profile, and the disconnection is attributed to degradation below 800 kOhm for an hour, influenced by rain-induced humidity, deeper degradation of polymer components in the photovoltaic module material, material corrosion, and temperature fluctuations. The starting condition for each inverter demands an operating insulation resistance of ≥ 3000 kOhm, considering a 300-volt open-circuit voltage and 1 kΩ/V insulation resistance by DIN VDE 0126-1-1. After optimizing the inverter's input-side insulation resistance, the system restarted despite a 20 mA capacitive leakage current, lower than the 22.7 mA first differential breaker sensitivity, as shown in Fig. 11, over about 3 hours.

Figure 8 details the performance anomalies of the second inverter regarding solar irradiation. Like the first inverter, it disconnects for about an hour between 8:00 and 9:00 due to insulation resistance degradation below 1500 kOhm, as depicted in Fig. 10 (Riso2). After adjusting the insulation resistance, the system disconnects again due to a 20 mA capacitive leakage current, in line with the value shown in Fig. 11 (Ileakage2), corresponding to the 20.1 mA sensitivity of the second differential breaker, with a response time of 11 ms.

Figure 8 presents performance anomalies concerning the solar irradiation of the third inverter in the morning. It disconnects for about four hours due to insulation resistance degradation below 100 kΩ, as shown in Fig. 10 (Riso3), due to rain, grounding issues in connection boxes, and poor grounding of multiple panels.

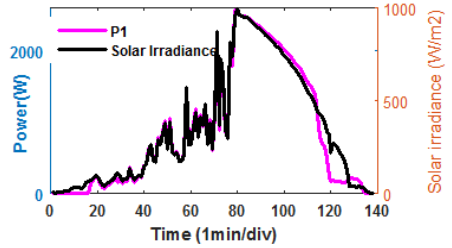

Fig. 7 – Performance of the first inverter.

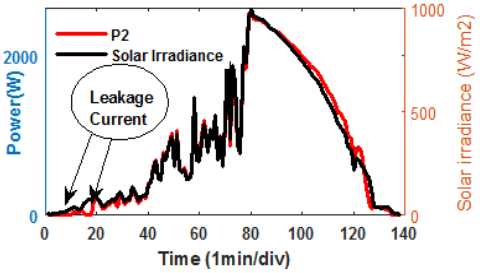

Fig. 8 – Performance of the second inverter.

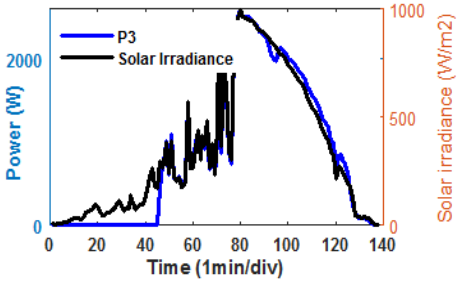

Fig. 9 – Performance of the third inverter.

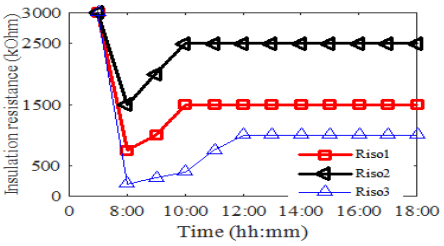

Fig. 10 – The variations of the insulation resistance at the input of the three inverters transformerless.

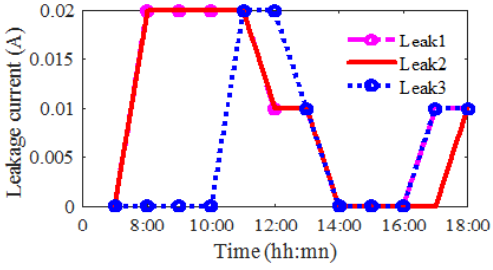

Fig. 11 – The variations of the capacitive leakage current of the three inverters transformer-less.

After optimizing the insulation resistance per DIN VDE 0126-1-1, the system restarted despite a 20 mA capacitive leakage current (Ileakage3), lower than the 22.7 mA sensitivity of the third differential breaker, as depicted in Fig. 11. Figure 12 shows the block diagram of the inverter's insulation resistance and leakage current using the DIN VDE 0126-1-1 standard.

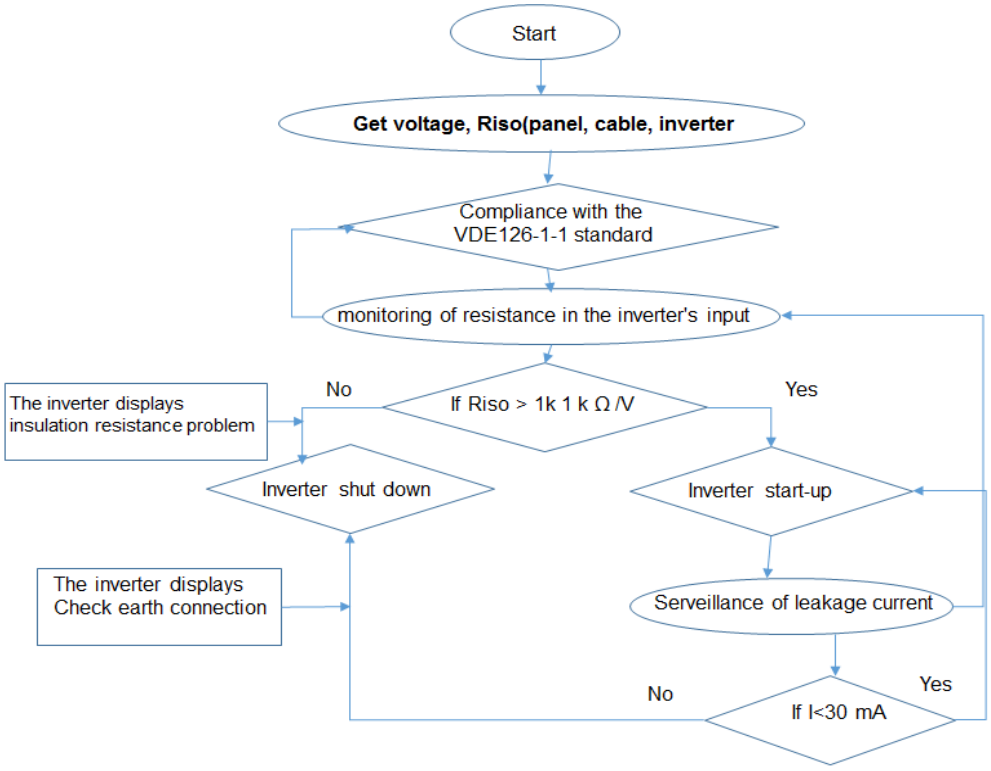

Fig. 12 – Block diagram of the inverter's insulation resistance and leakage current using the DIN VDE 0126-1-1 standard.

The insulation resistance and capacitive leakage current management are depicted in the organized structure of Fig. 9. A two-fold management strategy is proposed in this section. The first layer of analysis calculates and compares the resistance level of the module, cable, and inverter assembly by the standards of DIN-VDE-0126-1-1. If the Riso is below the authorized limit due to weather conditions such as rain, the control strategy is activated, preventing the inverter from starting and indicating an insulation resistance issue. If the Riso exceeds the standard, the inverter starts and applies the second control layer for capacitive leakage current. If the leakage current is below 30 mA, the system continues to operate normally. However, exceeding 30 mA could trigger protective devices, leading to the system shutdown, with the inverter displaying a message to check the grounding connection. This approach ensures proactive and effective management of critical aspects of electrical safety in photovoltaic systems.

7. **CONCLUSION**

Transformable PV inverters are pivotal components in contemporary grid-connected PV power generation systems. They boast superior power efficiency and lower current and voltage total harmonic distortion (THD) compared to their galvanically isolated counterparts. This study delves into the performance variations among three single-phase transformer-less inverters, examining efficiency, THD, insulation resistance at the inverter input, and capacitive leakage current.

In summary, our comprehensive investigation into insulation resistance (Riso) and capacitive leakage current management in photovoltaic systems underscores the importance of adhering to the VDE126-1-1 standard. Adhering to this rigorous standard, our research showcases a systematic and effective approach to evaluating Riso before grid integration and controlling capacitive leakage currents during system operation. The standard offers a precise normative framework that governs these phenomena' measurement, monitoring, and management, encompassing specific parameters related to modules, inverters, dc cables, and ground connections. Our study underscores the relevance and effectiveness of VDE126-1-1 as an indispensable tool, ensuring the reliability and safety of photovoltaic installations. This normative approach significantly advances photovoltaic system management, providing clear directives and precise criteria for optimal operation while adhering to the highest safety standards.

Received 1 February 2023

REFERENCES

1. T.H. Van, T.L. Van, T.M. Nguyen Thi, M.Q. Duong, G.N. Sava, *Improving the output of dc-dc converter by phase shift full bridge applied to renewable energy*, Rev. Roum. Sci. Techn.– Électrotechn. et Énerg., **66**, *3*, pp. 175–180 (2021).
2. H. Sridharan, S. Ramalingam, A. Jawahar, *Wide boost ratio in quasi-impedance network converter using switch voltage spike reduction technique*, Rev. Roum. Sci. Techn.– Électrotechn. et Énerg., **68**, *3*, pp. 259–265 (2023).
3. D. Roy, M. Singh, *Realization of a three-level neutral point clamped inverter using a novel region selection approach of bus clamping PWM for electric vehicle application*, Rev. Roum. Sci. Techn.– Électrotechn. et Énerg. **68**, *2*, pp. 139–145 (2023).
4. E. Melić, A. bosović, M. Musić. *Analysis of the impact of different distributed generator technologies on harmonic voltages*, Rev. Roum. Sci. Techn.– Électrotechn. et Énerg., **68**, *2*, pp. 146–151 (2023).
5. M.A. Ilie, D. Floricău, *Grid-connected photovoltaic systems with multilevel converters – modeling and analysis*, Rev. Roum. Sci. Techn.– Électrotechn. et Énerg., **68**, *1*, pp. 77–83 (2023).

6. I. Picioroaga, A. Tudose, D. Sidea, C. Bulac , L. Toma, *Power supply restoration in active distribution networks with high photovoltaic penetration based on soft open points,* Rev. Roum. Sci. Techn.– Électrotechn. et Énerg., **66**, *3*, pp. 181–186 (2021).
7. A. Boudghene Stambouli, Z. Khia, S. Flazi, Y. Kitamura, *A review on the renewable energy development in Algeria: current perspective, energy scenario and sustainability issues,* Renewable and Sustainable Energy Reviews., **16**, *7*, pp. 4445–4460 (2012)
8. I. Bendaas, A. Hadj Arab, B. Taghezouit, S. Bouchakour, I. N. Elghoul, S. Boulahchiche, S. Semaoui, S. Bouacha, A. *Razagui, Effect of a new smarts photovoltaic inverters connected with a distribution network in Algeria*, IEEE 6th International Symposium on New and Renewable Energy (SIENR), pp. 1–6, 2021.
9. M. Obi, R. Bass, *Trends and challenges of grid-connected photovoltaic systems – a review*, Renewable and Sustainable Energy Reviews., **58**, 1082–1094 (2016).
10. R. Ramesh, A.J. Dhanaseely, P. Pughazendiran, *Single phase transformer based inverter for nonlinear load application using pi controller*, Journal of Engineering Research and Applications, **4**, *3*, pp. 86–90 (2014).
11. S. Kirthiga, N.M. Jothi Swaroopan, *Highly reliable inverter topology with a novel soft computing technique to eliminate leakage current in grid-connected transformerless photovoltaic systems*, Computers And Electrical Engineering, **68**, pp. 1082–1094 (2018).
12. Technical information SMA, *Courants de fuite capacitifs pour le dimensionnement d'onduleurs sans transformateur Sunny Boy, Sunny Mini Central ET Sunny Tripower*, éditions 25.
13. W.Chen, X.Yang, W.Zhang, X.Song, *Leakage current calculation for PV inverter system based on a parasitic capacitor model*, IEEE Transactions on Power Electronics, **31**, *12*, pp. 8205–8217 (2016).
14. Z. Liao, C. Cao, D. Qiu, *Analysis on topology derivation of single-phase transformerless photovoltaic grid-connect inverters*, Optik., **182**, pp. 50–57 (2018).
15. Technical information SMA, *Résistance d'isolement (Riso) d'installations photovoltaïques sans séparation galvanique*.
16. DIN VDE V 0126-1-1 VDE V 0126-1-1, *Automatic disconnection device between a generator and the public low-voltage grid*, 2013.
17. J. Flicker, J. Johnson, M. Albers, G. Ball, *Recommendations for isolation monitor ground fault detectors on residential and utility-scale PV systems*, IEEE 42nd Photovoltaic Specialist Conference (PVSC). pp. 1–6, 2015.
18. R. Araneo, M. Mitolo, *Insulation resistance and failures of a high-power grid-connected photovoltaic installation: a case study*, IEEE Industry Applications Magazine, **27**, *3*, pp.16–22 (2021).
19. S. Bouacha,A. Malek,O. Benkraouda, A. Hadj Arab, A. Razagui, S. Boulahchiche, S. Semaoui, *Performance analysis of the first photovoltaic grid-connected system in Algeria*, Energy for Sustainable Development, **57**, pp. 1–11 (2020).